JOURNAL OF OPTOELECTRONICS AND ADVANCED MATERIALS Vol. 9, No. 12, December 2007, p. 3927 - 3932

Polyanion structure and mixing conditions - useful tools to tailor the characteristics of polyelectrolyte complex particles

E. S. DRAGAN*, M. MIHAI
"Petru Poni" Institute of Macromolecular Chemistry, Aleea Gr. Ghica Voda 41A, 700487 Iasi, Romania

---

The formation of polyelectrolyte complex particles, at a nanometer level, by the complexation between poly(diallyldimethyammonium chloride) and two ionic/nonionic random copolymers of sodium 2-acrylamido-2-methylpropanesulfonate with either t-butyl acrylamide, P($AMPS_{54}$-co-TBA_{46}), or methyl methacrylate, P($AMPS_{52}$-co-MM_{48}), is described in this study. Dynamic light scattering and atomic force microscopy were used to investigate the influence of the polyanion structure, molar mixing ratio and titrant addition rate on the shape, sizes and polydispersity of the complex nanoparticles.

(Received December 4, 2007; accepted December 4, 2007)

Keywords: Polyelectrolyte complex dispersions, Titrant addition rate, Dynamic light scattering, Atomic force microscopy

---

1. Introduction

In the field of polymeric materials, polyelectrolyte complexes (PEC) are of high relevance since they offer the possibility to combine physicochemical properties of at least two polyelectrolytes. The driving forces for PECs formation are the strong Coulombic interactions between oppositely charged polyelectrolytes leading to interpolymer ionic complexation and the simultaneous release of counterions. Other inter-macromolecular interactions may be involved in the formation of PEC structures such as hydrogen bonding, hydrophobic interactions, van der Waals forces, or dipole-charge transfer. PECs can be divided mainly into three different classes: soluble PEC, i.e. macroscopically homogeneous systems containing nanoscopic PEC aggregates [1,2]; turbid colloidal systems with suspended PEC particles in the transition range to phase separation [3-7]; two-phase systems of supernatant liquid and precipitated PEC [8,9]. The shape and structure of the formed PECs depend on the characteristics of the polyelectrolytes involved and on the solution and mixing conditions during formation, two borderline structure models, the non-ordered scrambled egg model and the highly ordered ladder model, being discussed in the literature [8]. Nowadays, interpolyelectrolyte complexes are considered as promising materials in a wide variety of applications, such as drug delivery systems [10], medical implants [11], multilayers [12,13], membranes with special separation properties [14], and microcapsules [15]. Furthermore, PECs as colloidal dispersions have been of great interest in chemical engineering, pharmaceutical and biological areas [3-5,16].

The investigation of the formation of stable colloidal PEC dispersions obtained by mixing poly (2 – sodium – 2 – acrylamido – 2 – methylpropane sulfonate) (NaPAMPS) or some random ionic/nonionic copolymers of AMPS, as polyanions (PA) with different strong polycations (PC), in a wide range between charges, was a major task in our previous studies [6,7,17,18]. For this purpose, the influence of polyion structure, concentration, addition order, and flow rate on the complex stoichiometry, particle size and colloidal stability were deeply followed by turbidimetry, colloidal titration, viscometry and dynamic light scattering (DLS). A special attention was paid to the correlation between the sizes of PEC nanoparticles, determined by DLS and atomic force microscopy (AFM), the benefits to use together these two methods to describe the morphology of the PEC dispersions being evidenced [19]. Formation of PEC particles using poly(diallyldimethyammonium chloride) (PDADMAC) and two copolymers of AMPS having almost the same content of the nonionic comonomer (t-butyl acrylamide, TBA, or methyl methacrylate, MM) is expected to be highly dependent on both polyelectrolyte characteristics (comonomer structure) and environmental parameters (titrant addition rate - TAR). In this paper, the polyanions were P($AMPS_{54}$-co-TBA_{46}) and P($AMPS_{52}$-co-MM_{48}), DLS and AFM being used to investigate the influence of these factors on the particle formation and characteristics, in a large range of molar mixing ratios between oppositely charged polyelectrolytes.

2. Experimental

Materials

PDADMAC, purchased from Aldrich, was used as received. The random copolymers of AMPS were synthesized by free-radical polymerization with AIBN as initiator [17].

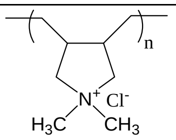

PDADMAC

M_w = 240000 g/mol

M_u = 162.70 g/charge

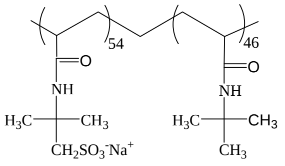

P($AMPS_{54}$-co-TBA_{46})

M_w = 175000 g/mol

M_u = 337.00 g/charge

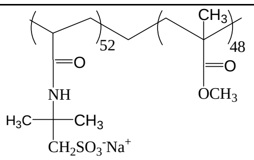

P($AMPS_{52}$-co-MM_{48})

M_w = 285000 g/mol

M_u = 322.05 g/charge

M_u – mass per charge

Sample preparation

Stable dispersions of PECs were prepared at room temperature (about 25 ^{o}C), by mixing aqueous solutions of oppositely charged polyelectrolytes in appropriate proportions. The amount of cationic polymer (having a constant concentration of 0.5 mM) was kept constant within a complex series, while the amount of anionic polymer (having a constant concentration of 5 mM) was varied according to the desired mixing molar ratio, n^-/n^+. The polyanion was added dropwise to the polycation, under magnetic stirring, with a constant TAR in the range 0.1 – 8.0 mL PA/mL PC. h. After mixing, the formed dispersions were stirred 60 min and were characterized after 24 h, by DLS.

For AFM investigations silicon wafers supports were used after carefully cleaning in two steps, as was described elsewhere [19]. Clean silicon wafers were immersed in PEC dispersions, identical with those used for DLS, for 20 min, then washed three times each 1 min in distilled water and finally air-dried at room temperature about 48 h.

Characterization methods

DLS measurements of PEC dispersions were carried out using a Zetasizer 3000 (Malvern Instruments, UK) equipped with a 10 mW He-Ne laser (633 nm) as a light source. The measurements were performed at a scattering angle of 90°, and the reported results are the average of two DLS independent measurements. The samples were kept at a constant temperature of 25 °C during all experiments. DLS measures the diffusion in particle dispersions, which can be interpreted using the Stokes-Einstein equation to yield the particle average hydrodynamic diameter, D_h:

$$D_h = k_B T / (3\pi\eta_s D)$$

where k_B is the Boltzmann constant, T is the absolute temperature (298 K), η_s is the dynamic viscosity of the solvent (for water 0.8872 cP), and D is the *z*-average translational diffusion coefficient.

To get information about the size distribution of PEC particles the polydispersity index, PI, was also included in the interpretation.

The shapes of PEC particles were examined by means of a Nanoscope IIIa Dimension 3100 SPM, (Digital Instruments Veeco Metrology Group, Woodbury, NY, USA), using a silicon probe Tap300, from BudgetSensors (Bulgaria). The topographic images were obtained using tapping mode, with a scan rate of 1 Hz, in ambient atmosphere, at room temperature. The PEC particle sizes were determined using the device software, which is designed to detect and measure the lateral dimensions of isolated particles on the sample surfaces, and to determine the minimum, maximum and mean diameter for the analyzed particles.

3. Results and discussion

3.1. DLS

DLS is a suitable method to monitor the formation of PEC particles as a function of the mixing molar ratio n^-/n^+, i.e., the molar ratio between anionic and cationic units. Figure 1 presents DLS results (D_h and PI) for both polyion pairs studied, as a function of the ratio between charges, for two TARs. A general characteristic revealed by DLS (Fig. 1A), before $n^-/n^+ = 0.9$, was the very slow increase in the particle sizes, from 128 nm to 133 nm, as the molar ratio increase, irrespective of polyion pair and TAR. As the mixing molar ratio was close to stoichiometry, i.e., for n^-/n^+ about 0.95, the loss of the charges in excess induced a secondary aggregation of the particles, probably through hydrophobic interactions, leading to an abruptly increase of the particle sizes, a very strong maximum followed by the decrease and level off of the D_h values being observed. For the same TAR (3.8 mL PA/mL PC. h), the value of the maximum was higher when the polyanion was P($AMPS_{54}$-co-TBA_{46}). The maximum disappeared after two weeks of storage (data not shown here), when bigger aggregates separated, only a part of the complex particles, which were protected against collision, remaining in supernatant.

PI describes the heterogeneity of the samples, values lower than 0.05 being ascribed to monodisperse particles and those higher than 0.2 indicating a broad size distribution. In this study, the values of PI (*Fig. 1B*) decreased by increasing the mixing molar ratio from 0.2 to 0.9, probably by the aggregation of the primary complex in bigger and more uniform particles, due to the consumption of the component in excess.

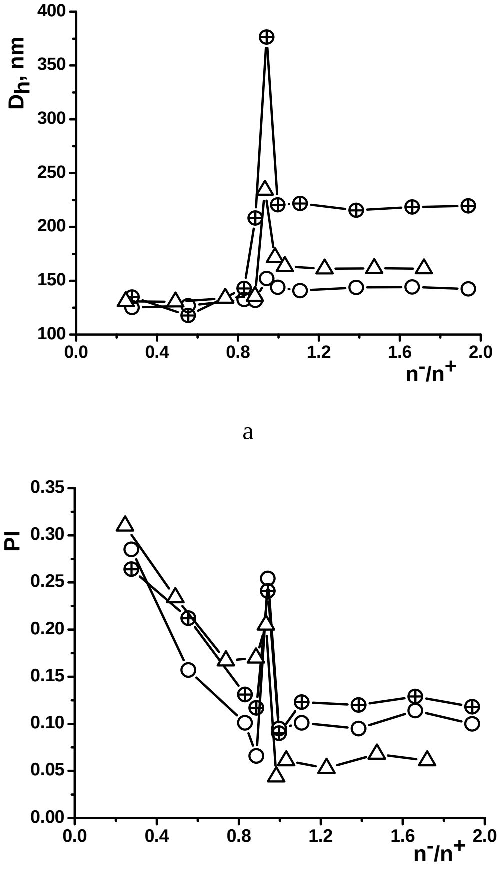

a

b

Fig. 1. D_h (A) and PI (B) of PA/PDADMAC dispersions as a function of the ratio between charges (n^-/n^+) at two different addition rates: (△) 3.8 mL P($AMPS_{54}$-co-TBA_{46})/mL PC.h; (○) 3.8 mL P($AMPS_{52}$-co-MM_{48})/mL PC.h; (⊗) 0.6 mL P($AMPS_{52}$-co-MM_{48})/mL PC.h.

Also, PI presents a maximum around the complex stoichiometry, which may be attributed to a lower stability of the complex dispersion just around the stoichiometric point, and level off after that at around 0.05 when TBA was the nonionic comonomer. PI values were around 0.1 for TAR = 3.8 mL PA/mL PC.h and 0.12 for TAR = 0.6 mL PA/mL PC.h, in the case of P($AMPS_{52}$-co-MM_{48}).

After the stoichiometry, when complex particles are stabilized by the PA in excess, both the particle sizes and the PI were almost independent of the molar ratio between charges.

The values of the particle sizes and their polydispersity as a function of TAR, for a constant ratio between charges, n^-/n^+ = 1.2, for both polyion pairs, were plotted in Fig. 2.

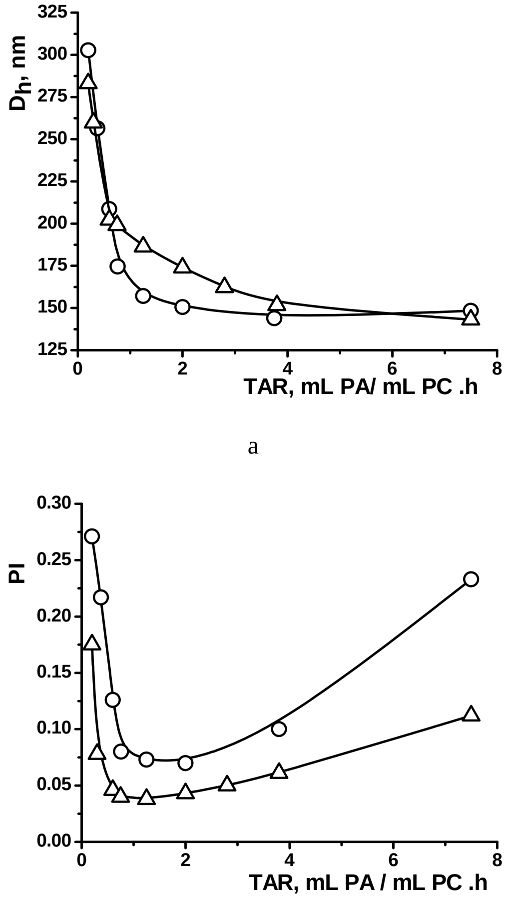

a

b

Fig. 2. D_h and PI of PEC particles as a function of titrant addition rate (TAR) at a constant molar ratio between charges, n^-/n^+, of 1.2: (△) P($AMPS_{54}$-co-TBA_{46})/ PDADMAC; (○) P($AMPS_{52}$-co-MM_{48}) PDADMAC.

As it was previously observed for other systems [7,17,19], TAR is a major parameter affecting the dimension of the complexes, higher TAR leading to smaller particles. Fig. 2a show that the influence of the polyanion structure on the PEC sizes was strongly manifested when TAR was between 0.6 and 4 mL PA/mL PC.h, in this case the higher particles being obtained with P($AMPS_{54}$-co-TBA_{46}) as polyanion. Out of this TAR domain, the particles sizes were almost the same, for both polyion pairs. The influence of polyanion structure on the PI, as a function of TAR, was stronger when P($AMPS_{52}$-co-MM_{48}) was used, an abrupt increase of PI being found when TAR was higher than 2 mL PA/mL PC.h and smaller than 0.6 mL PA/mL PC.h, almost monodisperse particles being formed with P($AMPS_{54}$-co-TBA_{46}), for all TAR values higher than 0.6 mL PA/mL PC.h (Fig. 2b).

3.2. AFM

AFM is a powerful technique used to characterize surface topography and morphology of individual, ensembles and clusters of nanoparticles. One of the greatest advantages of AFM over traditional techniques, such as optical and electron microscopy, is that AFM directly produces three-dimensional (3D) images. In this work, AFM imaging has been applied to P(AMPS$_{52}$-co-MM$_{48}$)/PDADMAC dispersion in order to investigate structural aspects of these nanoparticles. Figures 3A and 3B presents the 2D and 3D amplitude images of the particles adsorbed and dried on the silicon wafers, formed at a TAR of 3.8 mL PA/mL PC.h, at two molar ratios between charges. The micrographs indicated that the adsorbed PECs appear as individual, dispersed particles and only some aggregated structures were formed. Even if the interaction with the silica surface could induce conformational changes in the individual PEC particles, due to electrostatic interactions during adsorption, after the air-drying procedure the PECs still display 3D structures, with almost spherical shapes. Very small particles were evident for the complex dispersion corresponding to a molar ratio $n^-/n^+ = 0.5$ (Fig. 3a). Close to the stoichiometry a broad range of sizes, ascribed to primary and secondary complexes, can be observed ($n^-/n^+ = 1.0$; Fig. 3b).

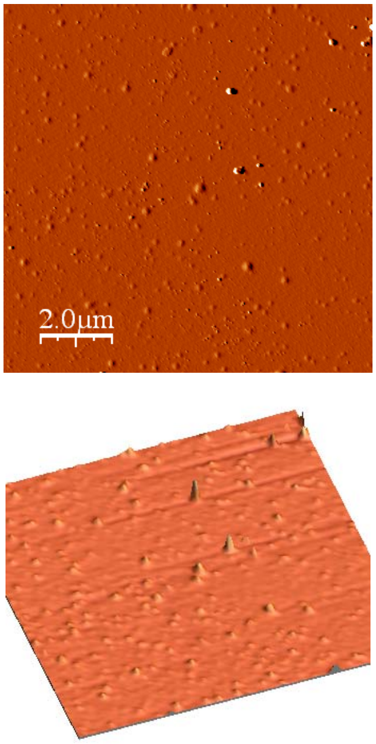

Fig. 3A. Tapping mode 2D and 3D amplitude AFM images of the P(AMPS$_{52}$-co-MM$_{48}$) / PDADMAC dispersion: n^-/n^+=0.5, TAR = 3.8 mL PA/mL PC.h.

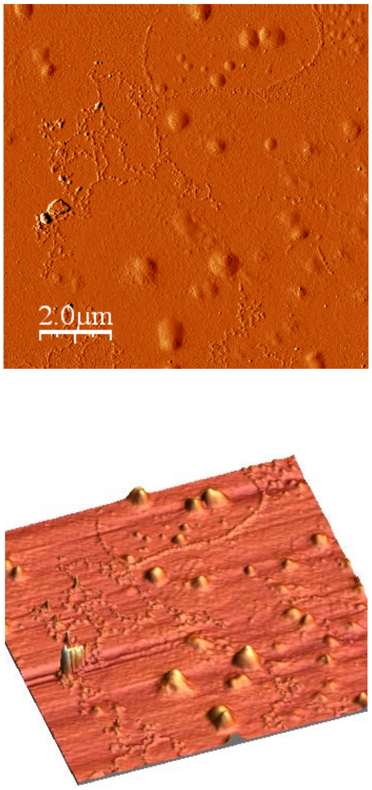

Fig. 3B. Tapping mode 2D and 3D amplitude AFM images of the P(AMPS$_{52}$-co-MM$_{48}$) / PDADMAC dispersion: n^-/n^+=1.0 , TAR = 3.8 mL PA/mL PC.h.

AFM was also used to evidence the influence of TAR on the particle size and shape, as well as on the size distribution. For this purpose, P(AMPS$_{52}$-co-MM$_{48}$)/PDADMAC particles prepared with different TAR, at a constant molar ratio between charges n^-/n^+ = 1.2, were examined (Figs. 4A, 4B and 4C). The trend found by DLS was confirmed in the AFM images: (1) when TAR was very slow (0.2 mL PA/mL PC.h, Fig. 4A) the particles aggregation through hydrophobic interactions led to the increase of the particle sizes, part of them being connected by each other in an irregular manner; (2) individual particles, with a compact core surrounded by a thick and fluffy coat were evidenced at TAR = 1.2 mL PA/mL PC.h (Fig. 4B), somehow similar with the shape of the particles presented in Fig. 3B; (3) at very high TAR (7.0 mL PA/mL PC.h, Fig. 4C), small particles were observed, with a compact structure. The high polydispersity index evidenced by DLS measurements is supporting by AFM, the adsorption of PEC particles resulted in an inhomogeneous mixture of smaller and bigger particles, irrespective of TAR.

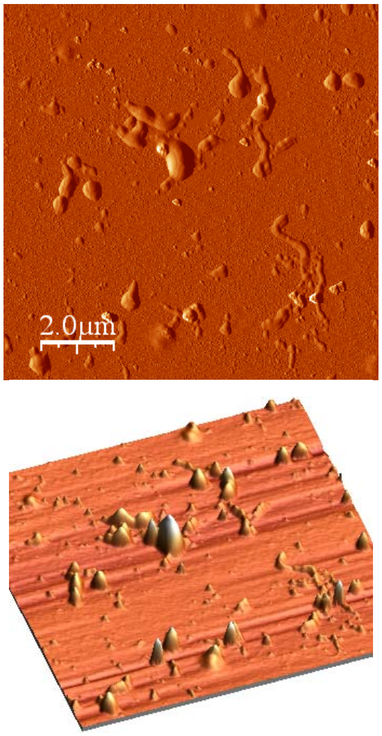

Fig. 4A. Tapping mode 2D and 3D amplitude AFM images of the $P(AMPS_{52}\text{-}co\text{-}MM_{48})$ */ PDADMAC dispersion;* $n^-/n^+=1.2$*, TAR =0.2 mL PA/mL PC.h.*

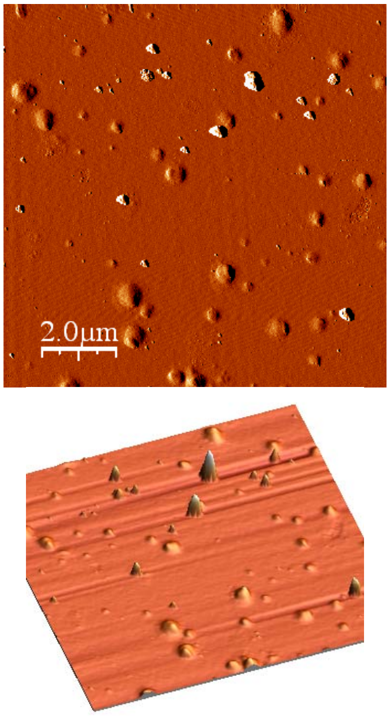

Fig. 4B. Tapping mode 2D and 3D amplitude AFM laufenimages of the $P(AMPS_{52}\text{-}co\text{-}MM_{48})$ */ PDADMAC dispersion;* $n^-/n^+=1.2$*, TAR =1.2 mL PA/mL PC.h.*

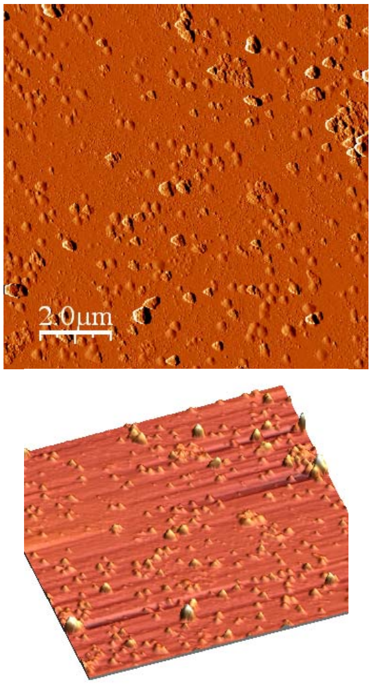

Fig. 4C. Tapping mode 2D and 3D amplitude AFM images of the $P(AMPS_{52}\text{-}co\text{-}MM_{48})$ */ PDADMAC dispersion;* $n^-/n^+=1.2$*, TAR =7 mL PA/mL PC.h.*

To compare the AFM data with DLS results, the sizes of about 50 individual PEC particles adsorbed on the silicon substrate were measured directly from AFM topographic images, using the device software. AFM observations were repeated on different areas of the same sample. The results obtained for the polyanion pair $P(AMPS_{52}\text{-co-}MM_{48})$/PDADMAC, using each of these methods are collected in Table 1.

Table 1. Minimum (d_{min})*, medium* (d_{med}) *and maximum* (d_{max}) *diameter determined by AFM and* D_h *measured by DLS for the* $P(AMPS_{52}\text{-}co\text{-}MM_{48})$*/ PDADMAC complex particles, at diferent TAR (mL PA/mL PC.h) and* n^-/n^+*.*

TAR	n^-/n^+	AFM			DLS	Fig
		d_{min}, nm	d_{med}, nm	d_{max}, nm	$D_{h,}$ nm	
3.8	0.5	22	93	322	116	1, 3A
3.8	1.0	42	139	464	148	1, 3B
0.2	1.2	22	290	1031	303	2, 4A
1.2	1.2	42	142	511	157	2, 4B
7.0	1.2	22	127	359	140	2, 4C

As Table 1 shows, there is often a discrepancy between AFM and DLS measurements, namely the medium particle sizes of the complex nanoparticles measured by AFM were always lower than those measured by DLS, both before and after the complex stoichiometry. These differences were also evidenced for other systems [4,19,20] and are attributed to factors associated with the operative conditions of each measurements: AFM provides the size of dehydrated particles and DLS measurements yield an ensemble average of the particle size in solution.

4. Conclusions

DLS and AFM have been used as complementary methods to describe the morphology of some PEC dispersions prepared with PDADMAC and two ionic/nonionic random copolymers of AMPS, P($AMPS_{54}$-co-TBA_{46}) or P($AMPS_{52}$-co-MM_{48}), as a function of the polyanion structure, the molar ratio between charges and TAR. The average sizes determined from the AFM images analysis are smaller than hydrodynamic particle diameter, D_h, determined by DLS. Compared to the image analysis of AFM micrographs, DLS is a very fast and statistically secure method for characterizing dispersed particle distributions. However, large particles are more easily detected using DLS and even a very small number of large particles leads to a considerable change in the obtained size distribution. Advantages of AFM are the direct evidence of the shape, size, and dispersity, which is not only an average value as that given by DLS.

References

[1] V. A. Kabanov, A. B. Zezin, Pure Appl. Chem. **56**, 343 (1984).
[2] E. Tsuchida, K. Abe, Adv. Polym. Sci. **45**, 1 (1982).
[3] H.-M. Buchhammer, G. Petzold, K. Lunkwitz, Langmuir **15**, 4306 (1999).
[4] M. Müller, B. Kessler, S. Richter, Langmuir **21**, 7044 (2005).
[5] D. Paneva, L. Mespouille, N. Manolova, P. Gegée, I. Rashkov, P. Dubois, J. Polym. Sci. Part A: Polym. Chem. **44**, 5468 (2006).
[6] E. S. Dragan, S. Schwarz, J. Polym. Sci. Part A: Polym. Chem. **42**, 2495 (2004).
[7] E. S. Dragan, S. Schwarz, J. Polym. Sci. Part A: Polym. Chem. **42**, 5244 (2004).
[8] B. Philipp, H. Dautzenberg, K. J. Linow, J. Koetz, W. Dawydoff, Prog. Polym. Sci. **14**, 91 (1989).
[9] S. Dragan, M. Cristea, In: Recent Research Developments in Polymer Science, Gayathri A. Ed.; Research Signpost, Trivandrum, India: Vol. 7, p. 149 (2003).
[10] C. Peniche, M. Fernandez, A. Gallardo, A. Lopez-Bravo, J. San Roman, Macromol. Biosci. **3**, 540 (2003).
[11] M. Sittinger, D. W. Hutmacher, M. V Risbud, Current Opinion Biotechnology **15**, 411 (2004).
[12] G. Decher, Science **277**, 1232 (1997).
[13] P. Bertrand, A. Jonas, A. Laschewsky, R. Legras, Macromol. Rapid Commun. **21**, 319 (2000).
[14] X. Feng, R. Pelton, M. Leduc, Ind. Eng. Chem. Res. **45**, 6665 (2006).
[15] A. A. Antipov, G. B. Suchorukov, Adv. Colloid. Inteface Sci. **111**, 49 (2004).
[16] S. Schwarz, E. S. Dragan, Macromol. Symp. **210**, 185 (2004).
[17] E. S. Dragan, M. Mihai, S. Schwarz, Colloids Surf. A. **290**, 213 (2006).
[18] M. Mihai, E. S. Dragan, Rev. Roum. Chem., in press.
[19] M. Mihai, E. S. Dragan, S. Schwarz, A. Janke, J. Phys. Chem. B, accepted.
[20] W. Ouyang, M. Müller, Macromol. Biosci. **6**, 929 (2006).

---

[*] Corresponding author: sdragan@icmpp.ro